OPEN ACCESS
IOP Publishing
Journal of Physics B: Atomic, Molecular and Optical Physics
J. Phys. B: At. Mol. Opt. Phys. **53** (2020) 125601 (5pp)
https://doi.org/10.1088/1361-6455/ab8049

Broadband terahertz solid-state emitter driven by Yb:YAG thin-disk oscillator

Gaia Barbiero[1,2], Haochuan Wang[1,2], Jonathan Brons[3,5], Bo-Han Chen[1,2], Vladimir Pervak[1] and Hanieh Fattahi[4,5]

[1] Fakultät für Physik, Ludwig-Maximilians-Universität München, Am Coulombwall 1, D-85748 Garching, Germany
[2] Max-Planck-Institut für Quantenoptik, Hans-Kopfermann-Str. 1, D-85748 Garching, Germany
[3] TRUMPF Laser GmbH, Aichhalder Straße 39, 78713 Schramberg, Germany
[4] Max-Planck-Institut für die Physik des Lichts, Staudtstr. 2, 91058 Erlangen, Germany

E-mail: hanieh.fattahi@mpl.mpg.de

Received 2 November 2019, revised 14 February 2020
Accepted for publication 16 March 2020
Published 27 May 2020

Abstract

We report on a table-top, high-power, terahertz (THz) solid-state emitter driven by few-cycle near-infrared pulses at 16 MHz repetition rate in gallium phosphide (GaP) crystals. Two external nonlinear multi-pass cells are used to shorten the output of a home-built, 100 W, 265 fs, 6.2 μJ Yb:YAG thin-disk oscillator, operating at 1030 nm, to 18 fs with 3.78 μJ pulse energy. The broadband spectrum of the THz driver allowed for the extension of the THz cutoff frequency to 5.7 THz at the dynamic range of 10^4. By employing the high-power Yb:YAG thin-disk oscillator, the low efficiency of the THz generation is circumvented, resulting in the generation of up to 100 μW, multi-octave THz pulses at 5 THz cutoff frequency in a 2 mm thick GaP crystal.

Keywords: broadband terahertz sources, nonlinear broadening, Kerr lens mode-locked Yb:YAG thin-disk oscillators, electro-optic sampling, multi-pass cells

(Some figures may appear in colour only in the online journal)

1. Introduction

Sources of intense, broadband, and coherent light in the terahertz (THz) spectral region (between 0.1 THz and 30 THz) operating at high average power and high repetition rates are seeing increasing interest in the ultrafast community as they benefit various applications, from non-destructive time-resolved molecular spectroscopy and imaging to THz communication and remote sensing [1].

Over the last 30 years, availability of the intense laser pulses based on chirped-pulse amplification [2] in solid-state lasers, in particular Ti:sapphire-based systems [3], accelerated the progress in the generation of ultra-broadband intense THz pulses based on ionizing gases [4]. Here the generated THz pulses do not suffer from phonon resonances or echoes unlike THz generation and detection in solids. However, the kilohertz (kHz) operation of these sources limits the measurement signal to noise ratio and increases the acquisition time. Therefore, novel, intense, broadband and coherent THz sources operating at a higher repetition rate, ideally in the megahertz (MHz) regime are required to decrease the measurement acquisition time and to enable resolving subtle processes and couplings that would never rise above the noise floor of current experiments.

Alternatively, THz pulses can be generated by optical rectification of few-cycle pulses in solids. The solid emitters have large gaps in their spectra due to phonon absorption and dispersion. However, they require driving pulses with lower peak intensities, in the order of tens of GW/cm^2, making them suitable candidates for the available laser technology. Diode-pumped Yb-doped oscillators have the promise to play an

[5] The authors current addresses are listed above.

important role in advancing solid-state THz emitters and detectors due to their higher average and peak power compared to other solid-state oscillators. Nowadays, they deliver pulses with tens of micro-joules of energy and hundreds of watts of average power [5, 6], reaching up to 25 MW peak power at 16.3 MHz repetition rate [7].

Yb-doped fiber amplifiers with hundreds of femtoseconds pulse duration and tens of watts of average power have been used to generate THz pulses with a cutoff frequency as high as 3 THz at 6.5 μW average power or 0.3 mW narrowband pulses [8–12]. However, in order to increase the bandwidth of the generated THz pulses, shorter pump pulses are desired. In 2018, Xu *et al* demonstrated THz pulses with negligible average power and 4 THz cutoff frequency by using 20 fs, 5.5 W pulses from an Yb fiber amplifier [13]. Later on, Paradis *et al* extended the bandwidth to 5 THz by using 50 fs, 4 W pulses from an Yb-doped thin-disk oscillator [14]. Meyer *et al* demonstrated the average power scaling of THz pulses to 78 μW at 2 THz cutoff frequency by employing 120 W, 580 fs pulses of an Yb-doped thin-disk oscillator [15]. Recently, Drs *et al* extended the amplitude of the THz spectrum to 5 THz at 0.3 mW average power by using a 95 fs Yb:YAG thin-disk oscillator [16].

In what follows we demonstrate scaling in average power and spectral bandwidth of THz pulses driven by 18 fs pulses via optical rectification in gallium phosphide (GaP) crystal. In our scheme, the output pulses of the oscillator are externally shortened to allow for extending the THz bandwidth, while the low efficiency of the processes is circumvented by employing a high-power Yb:YAG thin-disk oscillator operating at 16 MHz repetition rate. We demonstrate an increase in the spectral bandwidth of the generated broadband THz pulses to 5.7 THz cutoff frequency at 10 μW of average power, in a 0.2 mm thick GaP crystal, and to 5 THz cutoff frequency at 100 μW of average power, in a 2 mm thick GaP crystal.

2. Experimental setup

A home-built Kerr lens mode-locked Yb:YAG thin-disk oscillator is used to generate THz pulses. A 6 mm thick crystalline quartz plate is included in the laser cavity to achieve Kerr lens mode-locking, resulting in 265 fs pulses at 1030 nm. The oscillator operates in a reduced atmosphere (160 mbar of pressure) and delivers 6.2 μJ, 100 W pulses at 16 MHz repetition rates [17].

Two external nonlinear spectral broadening stages are developed to extend the spectral bandwidth of the oscillator's output and to satisfy the desired conditions for broadband THz generation. It is known that the interaction of intense laser pulses with materials with cubic nonlinearity results in self-phase modulation and generation of new spectral components. However, because of the uneven distribution of energy in a Gaussian beam profile, the beam quality after the self-phase modulation is severely degraded, limiting the achievable throughput efficiency [18]. To overcome this limitation, the B-integral per pass through the nonlinear medium should be kept below π while the small broadening factor can be

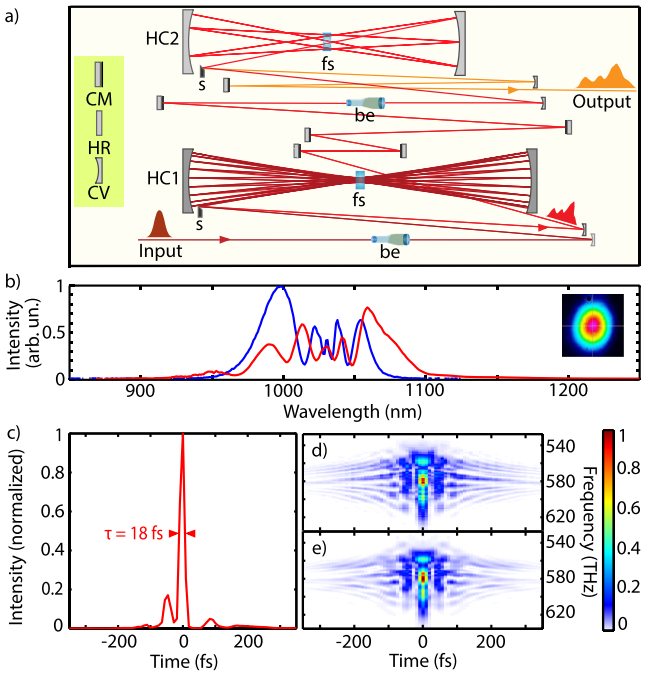

Figure 1. (a) Schematic of the cascaded nonlinear broadening setup (fs: fused silica, be: beam expander, HC: Herriott cell, s: scraper, CM: chirped mirror, HR: high reflective mirror, CV: curved mirror). (b) Output spectrum of the first (blue) and the second (red) broadening stage. The spectra are normalized to their energy ratio. The inset shows the output beam profile after the second stage. (c) Retrieved temporal profile of the output compressed pulses, corresponding to 18 fs duration at full width at half maximum. (d) The corresponding measured and (e) retrieved spectrograms.

circumvented by increasing the passes through the nonlinear medium in a wave-guide like multi-pass geometry [19–22]. In this scheme, the nonlinear medium is placed in the focal plane of a Herriott-type imaging cell (HC) with resonator stability. The beam is re-imaged after each pass to the medium and the induced temporal phase is compensated after each pass by using dispersive mirrors.

Figure 1(a) shows a schematic of the two consecutive HCs used in our system. In the first stage, 6.2 μJ pulses of the oscillator were sent to an HC containing two curved dispersive mirrors with radius of curvature of 300 mm, and group delay dispersion (GDD) of -160 fs^2 for 350 nm spectral bandwidth centered at 1030 nm. A 6.35 mm thick, anti-reflection-coated fused silica (FS) plate was used as the nonlinear medium. The output spectrum of the first HC after 38 passes through the medium is shown in figure 1(b) (blue curve) corresponding to an 11.3-fold spectral broadening and 82% optical efficiency. Increasing the number of passes at this stage does not lead to a higher factor of spectral broadening, due to the limited bandwidth of the dispersive mirrors of the HC and the accumulated residual linear and nonlinear phase from each round trip. The output pulses of the first stage were coupled out and compressed to 46 fs by using seven additional dispersive mirrors, compensating the total residual dispersion of 840 fs^2 around 1030 nm.

Afterwards, the compressed pulses were sent to a second HC containing two concave dispersive mirrors with radius of

curvature 250 mm, and a 6.35 mm thick, anti-reflection-coated FS plate as the nonlinear medium. The concave mirrors at this stage have a GDD of -120 fs^2 for 600 nm spectral bandwidth. The output spectrum after six passes through the nonlinear medium is shown in figure 1(b) (red curve). At this stage the residual accumulated linear and nonlinear phase is negligible as the number of passes is small. The output pulses were sent to a compressor containing three dispersive mirrors with -120 fs^2 GDD per bounce and were compressed to 18 fs. A home-built, frequency-resolved optical gating based on second harmonic generation (SHG-FROG) employing a 10 μm β-barium borate crystal was used to characterize the pulses (figure 1(c)).

The described frontend delivers 18 fs pulses with a total energy of 3.8 μJ, corresponding to 60% optical efficiency.

THz transients were generated via optical rectification of the femtosecond near-infrared pulses in an uncoated 110-cut GaP crystal in a collinear phase-matching geometry, where n_g(pump) $=$ n(THz), i.e. the group velocity of the pump pulse is equal to the phase velocity of the emitted THz wave [23].

The 3.8 μJ, 18 fs pulses at 1030 nm were focused using a convex lens with 250 mm focal length. The GaP was placed before the focus of the laser at a beam diameter of 700 μm ($1/e^2$), corresponding to 97 GW/cm^2 peak intensity and a fluence of 2 mJ/cm^2 at an average power of 60.5 W for THz generation.

The generated THz beam was then collimated using a 2″ off-axis bare-gold-coated, pierced parabolic mirror with a focal length of 101.6 mm. The pump beam was transmitted through the hole in the center of the parabolic mirror and the reflected THz beam was passed through a Teflon filter to block the residual of the pump beam, and afterwards was redirected towards an electro-optic sampling (EOS) setup for detection.

Less than 1% of the fundamental beam before the THz generation stage was separated by a calcium fluoride plate and used as the probe beam for the EOS. The 18 fs pulses offer sufficient temporal resolution to resolve the highest theoretically predicted frequency of the THz pulses. A second 2″ off-axis bare-gold-coated, pierced, parabolic mirror with a focal length of 50.8 mm was used to recombine the probe and the THz beams and also to focus the THz beam into the EOS nonlinear crystal. The two beams were overlapped and focused into a 0.15 mm thick, 110-cut GaP crystal, while their relative delay was controlled by a motorized linear stage (Physik Instrumente Q-545). Due to the Pockels effect, the refractive index of the GaP is modified in proportion to the strength of the THz field, which can be resolved by detecting the changes in the polarization state of the probe beam.

The polarization was then evaluated by using an ellipsometer consisting of a quarter-wave plate (Thorlabs AQWP10M-980), Wollaston prism (Thorlabs WP10), and a balanced photodiode (Thorlabs PDB210A). The THz pulses were mechanically chopped at a frequency of 1 kHz. The mechanical chopper was placed at a focus of THz beam generated using a second pair of bare-gold-coated parabolic mirrors prior to the EOS setup. A Stanford SR830 lock-in amplifier was used to read the output of the balanced photodiode. In addition to the electric field of the THz pulses, the THz power was measured by a commercial Golay cell detector (Tydex GC-1P) at the position of the EOS crystal.

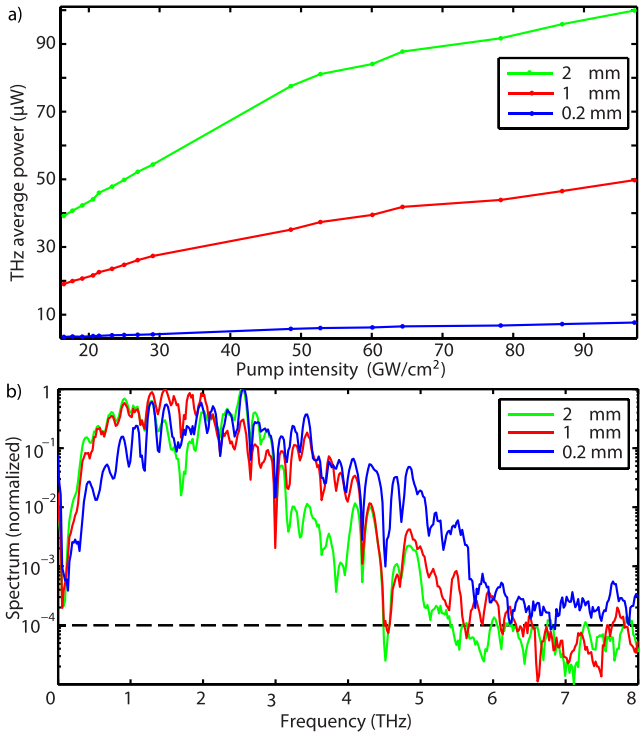

Figure 2. (a) Power of the generated THz pulses versus the peak intensity of pump pulses for different thicknesses of GaP, obtained under ambient conditions. (b) Power spectra of the generated THz pulses at 97 GW/cm^2 pump peak intensity for different thicknesses of GaP.

3. Conclusions

Figure 2 shows the measured average power and the retrieved spectra of the generated THz pulses in 2 mm, 1 mm, and 0.2 mm thick GaP crystal. In the power calculation, power losses caused by the transmission of the Teflon filter and the reflections of the parabolic mirrors are taken into account. For the 2 mm GaP and at pump peak intensities beyond 70 GW/cm^2, the dispersion for the few-cycle pump pulses and the temporal walk-off between the generated THz pulses and the pump pulses become more prominent, resulting in a different behavior (figure 2(a)) [24, 25].

The normalized spectra for three different thicknesses of GaP are compared in figure 2(b). As shown, the cutoff frequency of THz pulses for the 0.2 mm GaP extends to 5.7 THz, taking the dynamic range of 10^4 into account. It is noticeable that at the maximum pump power, no extra cooling of the GaP crystal was required even after hours of radiation.

Figure 3 shows the resolved electric field of the THz transient and its corresponding retrieved spectrum for the 0.2 mm thick GaP crystal, delivering the broadest THz spectrum in our

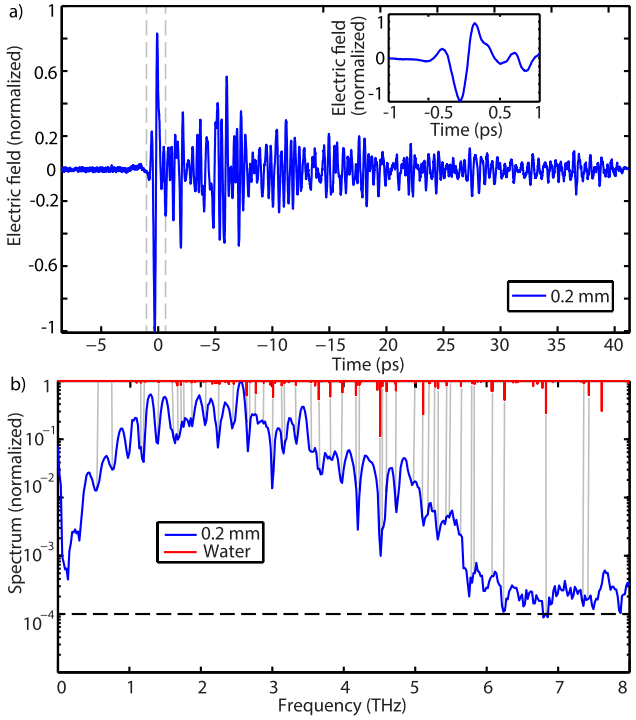

Figure 3. (a) THz transient electric field generated in a 0.2 mm thick GaP crystal measured by electro-optic sampling containing a 0.15 mm thick GaP crystal. The free induction decay resulting from the absorption of the generated THz pulses by water vapor molecules can be observed at the trailing edge of the waveform. The experiment is performed in a room with 46% humidity. Inset: zoom of the main pulse. (b) Retrieved THz spectrum of the waveform shown in panel (a). The red lines show water absorption lines obtained from HITRAN.

study. Each data set is acquired in a 10 min scan with a 30 ms integration constant. Due to the relatively high humidity of the laboratory ($\approx 46\%$), absorption of the THz pulses by water vapor molecules [26] in air can be resolved in the trailing edge of the THz transient in the time domain and appears as several dips in the retrieved spectrum, which are in good agreement with the water absorption lines from the HITRAN database (red curve in figure 3(b)) [27]. As can be seen, the water vapor lines are reliably detected with 10 GHz resolution. The large amplitude of the free induction decay at the trailing edge of the pulse suggests high absorption of the generated THz pulses by water molecules. Therefore, decreasing vapor water molecules in the system would lead to higher output power of the generated THz transients.

In conclusion, driving THz solid-state emitters by few-cycle pulses generated externally from high repetition rate, Yb:YAG, thin-disk oscillators is a promising method for producing broadband THz pulses with wide application in THz imaging and spectroscopy at rapid acquisition time. In this letter, we demonstrated the pulse shortening of 6 μJ, 265 fs pulses from a Kerr lens, mode-locked Yb:YAG oscillator in an external, cascaded, nonlinear stage based on self-phase modulation to 3.8 μJ, 18 fs pulses at 16 MHz repetition rate. By using the few-cycle pulses to pump GaP as a solid-state emitter, a broadband THz spectrum with a cutoff frequency as high as 5.7 THz and average power of 10 μW is generated. Scaling the thickness of the crystal to 2 mm results in the generation of 100 μW THz pulses with a lower cutoff frequency at 5 THz, corresponding to 6 pJ pulse energy. The observed cutoff in this experiment is in good agreement with the calculation in [28]. It can be seen that at higher conversion efficiencies the effects of dispersion of pump pulses, temporal walk-off between the interacting beams, and spectral red-shifting become prominent, and slow down the slope of the efficiency curve. The observed strong absorption of THz pulses with water vapor molecules suggests that higher output power can be achieved by reducing the humidity in the system. Moreover, the resolved absorption lines of water prove the dynamic range, robustness, and stability of the system as a spectroscopy module.

Acknowledgments

This project was funded by the Center of Advanced Laser Application (CALA). Hanieh Fattahi is grateful for the MINERVA fast track scholarship from the Max Planck Society. The authors would like to thank Ayman Alismail, Leon Helms, Christina Hofer, Ferenc Krausz, and Enrico Ridente for their support.

ORCID iDs

Gaia Barbiero https://orcid.org/0000-0002-9001-3002
Haochuan Wang https://orcid.org/0000-0002-1863-9553
Hanieh Fattahi https://orcid.org/0000-0002-6485-529X

References

[1] Dhillon S S *et al* 2017 *J. Phys. D: Appl. Phys.* **50** 043001
[2] Strickland D and Mourou G 1985 *Opt. Commun.* **55** 447–9
[3] Chu Y *et al* 2013 *Opt. Express* **21** 29231
[4] Karpowicz N *et al* 2008 *Appl. Phys. Lett.* **92** 011131
[5] Fattahi H *et al* 2014 *Optica* **1** 45–63
[6] Hua Y *et al* 2018 *Opt. Lett.* **43** 1686
[7] Saraceno C J, Emaury F, Schriber C, Hoffmann M, Golling M, Südmeyer T and Keller U 2014 *Opt. Lett.* **39** 9–12
[8] Li J *et al* 2014 *Appl. Phys. Lett.* **104** 031117
[9] Chang G, Divin C J, Liu C H, Williamson S L, Galvanauskas A and Norris T B 2006 *Opt. Express* **14** 7909
[10] Hoffmann M C, Yeh K L, Hwang H Y, Sosnowski T S, Prall B S, Hebling J and Nelson K A 2008 *Appl. Phys. Lett.* **93** 141107
[11] Cui W, Schiff-Kearn A W, Zhang E, Couture N, Tani F, Novoa D, Russell P S and Ménard J M 2018 *APL Photonics* **3** 111301
[12] Meyer F, Hekmat N, Vogel T, Omar A, Mansourzadeh S, Fobbe F, Hoffmann M, Wang Y and Saraceno C J 2019 *Opt. Express* **27** 30340–9
[13] Xu J, Globisch B, Hofer C, Lilienfein N, Butler T, Karpowicz N and Pupeza I 2018 *J. Phys. B: At. Mol. Opt. Phys.* **51** 154002
[14] Paradis C, Drs J, Modsching N, Razskazovskaya O, Meyer F, Kränkel C, Saraceno C J, Wittwer V J and Südmeyer T 2018 *Opt. Express* **26** 26377
[15] Meyer F, Hekmat N, Mansourzadeh S, Fobbe F, Aslani F, Hoffmann M and Saraceno C J 2018 *Opt. Lett.* **43** 5909

[16] Drs J, Modsching N, Paradis C, Kränkel C, Wittwer V J, Razskazovskaya O and Südmeyer T 2019 *J. Opt. Soc. Am.* B **36** 3039–45
[17] Brons J, Pervak V, Bauer D, Sutter D, Pronin O and Krausz F 2016 *Opt. Lett.* **41** 3567–70
[18] Seidel M, Arisholm G, Brons J, Pervak V and Pronin O 2016 *Opt. Express* **24** 9412–28
[19] Weitenberg J, Vernaleken A, Schulte J, Ozawa A, Sartorius T, Pervak V, Hoffmann H D, Udem T, Russbüldt P and Hänsch T W 2017 *Opt. Express* **25** 20502–10
[20] Weitenberg J, Saule T, Schulte J and Rusbuldt P 2017 *IEEE J. Quantum Electron.* **53** 1–4
[21] Schulte J, Sartorius T, Weitenberg J, Vernaleken A and Russbueldt P 2016 *Opt. Lett.* **41** 4511–4
[22] Fritsch K, Poetzlberger M, Pervak V, Brons J and Pronin O 2018 *Opt. Lett.* **43** 4643
[23] Bakker H J, Cho G C, Kurz H, Wu Q and Zhang X C 1998 *J. Opt. Soc. Am.* B **15** 1795–801
[24] Hoffmann M C, Yeh K L, Hebling J and Nelson K A 2007 *Opt. Express* **15** 11706–13
[25] Fattahi H, Schwarz A, Keiber S and Karpowicz N 2013 *Opt. Lett.* **38** 4216–9
[26] van Exter M, Fattinger C and Grischkowsky D 1989 *Opt. Lett.* **14** 1128
[27] Gordon I *et al* 2017 *J. Quant. Spectrosc. Radiat. Transfer* **203** 3–69
[28] Leitenstorfer A, Hunsche S, Shah J, Nuss M C and Knox W H 1999 *Appl. Phys. Lett.* **74** 1516–8